Organic electrochemical transistor-based channel dimension-independent single-strand wearable sweat sensors

Youngseok Kim[1], Taekyung Lim[2], Chi-Hyeong Kim[1], Chang Su Yeo[3], Keumyoung Seo[2], Seong-Min Kim[1], Jiwoong Kim[1], Sang Yoon Park[3], Sanghyun Ju[2] and Myung-Han Yoon[1]

Abstract
Despite the great potential of polymer microfibers in human-friendly wearable electronics, most previous polymeric electronics have been limited to thin-film-based devices due to practical difficulties in fabricating microfibrillar devices, as well as defining the active channel dimensions in a reproducible manner. Herein, we report on conducting polymer microfiber-based organic electrochemical transistors (OECTs) and their application in single-strand fiber-type wearable ion concentration sensors. We developed a simple wet-spinning process to form very conductive poly(3,4-ethylenedioxythiophene):poly(styrene sulfonate) (PEDOT:PSS) microfibers using aqueous sulfuric acid solutions and carefully examined their electrical/electrochemical properties. In conjunction with fabricating substrate-free PEDOT:PSS microfiber-based OECT devices, the proposed novel characterization method demonstrated that the current variation ratio can be a reliable method for evaluating the device performance for sensing ion concentrations, regardless of the actual channel dimensions. Finally, we developed single-strand fiber-type skin-mountable OECTs by introducing a source-gate hybrid electrode and demonstrated that the resultant microfiber sensors can perform real-time repetitive measurements of the ion concentration in human sweat.

Introduction

Over the last several decades, field-effect transistors (FETs) have been widely used in various electronic devices, including integrated circuits, display panels, radiofrequency identification readers, and wearable/implantable biomedical devices, benefiting from the efficient current/voltage amplification modulated by the gate bias. Meanwhile, various types of active channel materials have been developed for FETs, ranging from single crystalline semiconductors (e.g., silicon, germanium, and gallium arsenide) to vacuum-deposited hydrogenated amorphous silicon and various metal oxides and, more recently, to two-dimensional or nanoscale materials (e.g., graphene, carbon nanotubes, and molybdenum disulfide). In parallel, organic electronic materials, such as small molecule semiconductors and conducting polymers, have also been intensively investigated to meet unconventional demands, for instance, tunable electrical/optical properties, mechanical flexibility, large-area solution processability, biocompatibility, and so on.

Recently, organic electrochemical transistors (OECTs) have been developed as a special modality of organic FETs. In OECTs, conducting polymers are typically utilized as the active channel layer, where the source-to-drain current is efficiently modulated by an in-situ doping/dedoping process in the presence of small mobile ions. The unique characteristics of OECTs, for instance, compatibility with aqueous environments[1,2]

Correspondence: Sanghyun Ju (shju@kgu.ac.kr) or Myung-Han Yoon (mhyoon@gist.ac.kr)
[1]School of Materials Science and Engineering, Gwangju Institute of Science and Technology, Gwangju 61005, Republic of Korea
[2]Department of Physics, Kyonggi University, Suwon, Gyeonggi-Do 16227, Republic of Korea
Full list of author information is available at the end of the article
These authors contributed equally: Youngseok Kim, Taekyung Lim

and stable device operation at low voltages even below 1 V, encouraged many researchers to apply OECTs to various types of bioelectronics and biosensors[3−5]. In particular, poly(3,4-ethylenedioxythiophene):poly(styrene sulfonate) (PEDOT:PSS) has been one of the most widely used materials for such purposes, from the interfacial coating in microelectrode arrays (MEAs)[6−10] to the active channel layer in OECTs[11−16], due to its high electrical conductivity and good redox properties[17−19]. Moreover, the decent ion permeability into the PEDOT:PSS layer has been employed to reduce the resultant electrode impedance by increasing the thickness of the deposited film[20,21]. In addition, the intrinsic high conductivity of PEDOT:PSS has enabled the realization of micrometer-scale OECTs with very high on-current (> 1 mA) and extraordinary transconductance (∼ 4 mS), which could lead to enhanced gains in amplifying bioelectrical signals[12] and improved sensitivities for detecting ions[22−24] and biomolecules[25−27]. Nonetheless, to our knowledge, most of the OECT devices reported in the previous literature have been demonstrated in the form of thin-film devices, which require supporting substrates based on either rigid (e.g., silicon, quartz, glass) or flexible materials (e.g., polyimide, polyethylene terephthalate, polyethylene naphthalate). In other words, the existence of underlying carrier substrates implies limited mechanical flexibility, facile fabrication, and human-unfriendly wearability, which impedes the full potential of organic electronics toward wearable and implantable bioelectronics. Although there exist a good number of previous reports on wet-spun conducting polymer microfibers[28−30], these fibers are formed mainly by polar organic solvent-based coagulation, which exhibits limited controllability for the microfiber diameter particularly below ∼ 20 μm and poor electrical conductivity (< 200 S/cm). Moreover, although various fiber-structured devices have been developed for wearable healthcare applications[31,32], it is not straightforward to fabricate microfiber-based transistors and define active channel dimensions (i.e., length, width, and fiber diameter), which predominantly determine the consequent device sensitivity and fabrication reproducibility in a reliable manner.

Herein, we report conducting polymer microfiber-based OECTs and their application to single-strand fiber-type channel dimension-independent wearable sensors for measuring ion concentrations in human sweat. The PEDOT:PSS microfibers were prepared by a simple wet-spinning process using a sulfuric acid-based coagulation medium, whereas their diameters and conductivities were effectively controlled. The microfiber-based substrate-free three-terminal OECT devices were fabricated via metal wiring, with the effect of the coagulation medium acidity on the corresponding OECT characteristics cautiously

examined in terms of the device response to various concentrations of aqueous ionic solutions in contact with the channel layer and the Ag/AgCl gate electrode. Then, a novel device characterization method was proposed relying on the current variation ratio, which is not affected by the actual channel dimensions, to define the microfiber OECT's ion-sensing capability in a reliable manner. Next, single-strand microfiber-based skin-mountable OECTs were fabricated by introducing a source-gate hybrid electrode, with their characteristics compared with those of the three-terminal microfiber OECTs. Finally, the ion-sensing capability of the single-strand microfiber-based OECT was examined using phosphate-buffered saline (PBS) solutions, artificial sweat, and human sweat samples to demonstrate the feasibility of applying this novel but very simple device platform based on free-standing conducting polymer microfibers to human-friendly wearable electronics.

Materials and methods
Materials

The PBS solution (10 × , Gibco) was diluted 10 times with deionized (DI) water, followed by adjustment of the pH to a value of 7. The artificial sweat was prepared by dissolving sodium chloride (1.25 g), L-histidine mono-hydrochloride monohydrate (0.125 g), and sodium phosphate dibasic (0.55 g) in DI water (250 mL). The preparation of artificial sweat was followed by ISO105-E04-2008; all chemicals were purchased from Sigma-Aldrich. Human sweat samples were collected from a volunteer (male, 33 years old) under humid (humidity > 85%) and hot (temperature ∼ 60 °C) conditions using paper wipes, and squeezed into a clean vial. Subsequently, the supernatant was collected and utilized for ion-sensing experiments.

Preparation of the PEDOT:PSS microfibers

PEDOT:PSS microfibers were prepared by the conventional wet-spinning process, followed by rinsing and drying. Briefly, commercially available PEDOT:PSS solution (PH1000, Heraeus) was concentrated with a rotary evaporator (HS-2005V-N, Hahnshin Scientific), resulting in a solid concentration of approximately 2.0–2.5 wt.%, and then filtered with a syringe filter (17593, Sartorius) before wet spinning. Next, the PEDOT:PSS solution was injected into the acidic coagulation medium (20, 40, 60, 80, or 100 volume% of sulfuric acid in water, OCI, EP grade), with an injection rate through a standard stainless-steel syringe needle (17 gauge) fixed at 15 mL/h. The blackish microfibers were formed immediately after injection and left in the given coagulation medium for 3 h, followed by rinsing with acetone and DI water, successively, for 30 min, and drying in a vacuum oven (120 °C) for 15 min.

Table 1 Geometrical and electrical properties of PEDOT:PSS microfibers prepared with various sulfuric acid solutions

Conc. of coagulation bath (vol. %)	Cross-sectional area (10^{-5} cm^2)	Resistance per unit length (Ω/cm)	Conductivity (S/cm)
20	12.3 ± 1.06	25.9 ± 2.92	318.0 ± 36.9
40	11.1 ± 0.39	21.1 ± 0.84	428.8 ± 16.7
60	10.1 ± 0.23	16.2 ± 1.12	614.8 ± 40.2
80	5.7 ± 0.13	24.6 ± 1.35	713.0 ± 37.4
100	3.9 ± 0.84	26.3 ± 0.19	968.4 ± 6.87

Characterization of the PEDOT:PSS microfibers

The overall morphology of PEDOT:PSS microfibers, including their cross-sectional areas, was imaged using field emission scanning electron microscopy (FE-SEM, JSM-7500F, JEOL). Regarding the cross-sectional area measurement, a given PEDOT:PSS microfiber was broken in liquid nitrogen and the exposed cross-section imaged using FE-SEM, followed by calculation of the actual cross-sectional area using ImageJ software. The electrical resistance of the microfibers was measured by the conventional four-point-probe method (at a current bias of 100 μA) using a source meter (Keithley 2400), with the corresponding electrical conductivities calculated using the cross-sectional areas and electrical resistance (Table 1).

Fabrication and characterization of the three-terminal microfibrillar OECT for ion sensing

For OECT fabrication, a PEDOT:PSS microfiber was connected with copper wires using Ag epoxy (CW2400, Chemtronics) for source and drain connections, with an active PEDOT:PSS channel length of approximately 5–7 mm defined by passivating the non-channel PEDOT:PSS regions and the copper lead wires with dielectric epoxy (F-301, Alteco) for electrical insulation. Note that Ag epoxy enabled good mechanical adhesion sufficient for low contact resistance and good repeatability/reproducibility for sample preparation and electrical/electrochemical measurements, even in contact with water. Next, an aqueous electrolyte reservoir was defined using an acrylic tube (25 mm diameter) and a microscope slide (S9213, Matsunami). The Ag/AgCl gate electrode was used after chlorinating an Ag wire (0.127 mm diameter, 99.9%, Alfa Aesar) with 4% sodium hypochlorite solution for 10 min.

The OECT transfer characteristics were obtained with a parameter analyzer (Keithley 4200). The pinch-off voltage was extracted from the transfer curve for the OECT in contact with 100 mM NaCl solution in the saturation region ($V_D = -0.6$, $V_G = -0.8$–0.8 V), with the corresponding hole density estimated from the volumetric capacitance and pinch-off voltage. The volumetric capacitances of the PEDOT:PSS fibers were extracted from the electrochemical impedance analysis data in the frequency range from 0.1 to 1 kHz at 0.0125 V_{pp} (PGSTAT 302 N, Metrohm-Autolab) after fitting with the appropriate equivalent circuit model.

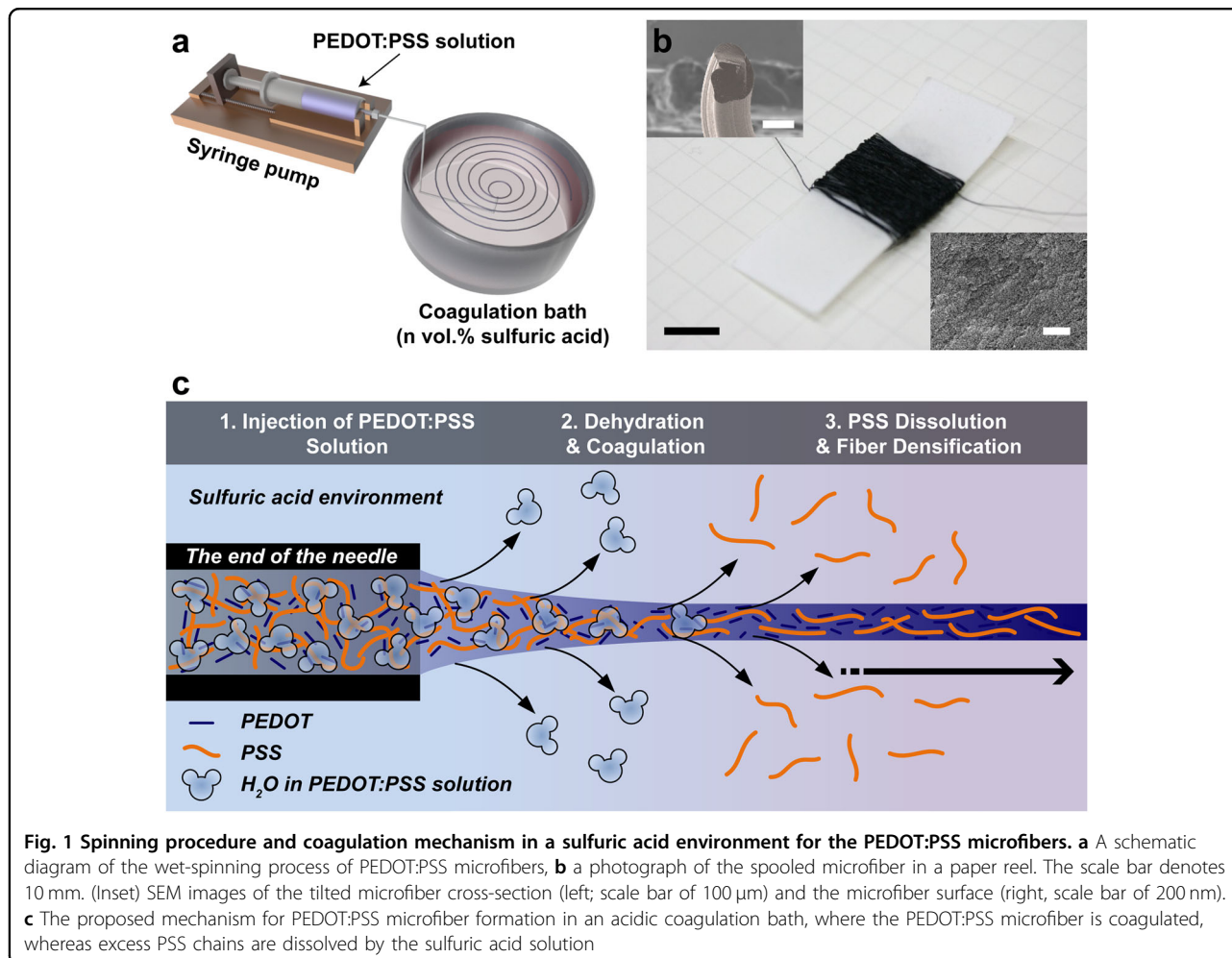## Fabrication of single-strand OECT-based ion sensors

Each end of the PEDOT:PSS microfiber was electrically connected with a silver wire using an Ag epoxy as described above. The Ag-PEDOT:PSS-Ag strand was passivated by spray coating the poly(methyl methacrylate) (PMMA) solution (Sigma-Aldrich, M.W = 120,000, 30 mg/mL in toluene) through a stencil mask except for the PEDOT:PSS OECT channel and the Ag epoxy source-gate junction, followed by curing in a vacuum oven at 150 °C for 30 min. Finally, the unpassivated Ag epoxy junction was chlorinated with a drop of sodium hypochlorite solution as described above.

Sensing characterizations of microfiber OECTs

For three-terminal devices, the source and drain electrodes of the microfiber OECT were electrically connected with a source meter and the current variation recorded at $V_D = -0.1$ V, whereas the gate bias was applied onto the Ag/AgCl gate electrode immersed in the aqueous electrolyte (NaCl) reservoir. During the measurement, a fresh electrolyte solution (∼ 5 mL) was injected into the reservoir, and removed by a suction tube for solution replacement. For two-terminal devices, the source-gate hybrid and drain electrodes of the microfiber OECT were electrically connected with the same source meter and the current was measured, whereas –0.1 V was applied onto the drain electrode with a time interval of 5 s. Note that all current measurements (in response to the aqueous electrolyte change) were performed under the (quasi) steady-state condition, which was defined as the moment when the electrochemical gate current becomes sufficiently negligible below ∼ 0.5 μA.

Measurement of ion concentrations in PBS, artificial sweat, and human sweat samples

The ion-sensing scheme is identical to that used for the above-mentioned electrical characterization of two-terminal OECT devices. First, the reference current was set using 1 mM NaCl solution, whereas the drain voltage was set at –0.1 V. After injecting an aqueous electrolyte sample into the reservoir, the drain current was recorded. The total cation concentration was calculated using the sensitivity (S) and reference current (I_{D0}) (Eq. 2, Fig. 5c), and then compared with the concentration measured by ion chromatography-inductively coupled plasma (IC-ICP)

Fig. 1 Spinning procedure and coagulation mechanism in a sulfuric acid environment for the PEDOT:PSS microfibers. a A schematic diagram of the wet-spinning process of PEDOT:PSS microfibers, **b** a photograph of the spooled microfiber in a paper reel. The scale bar denotes 10 mm. (Inset) SEM images of the tilted microfiber cross-section (left; scale bar of 100 μm) and the microfiber surface (right, scale bar of 200 nm). **c** The proposed mechanism for PEDOT:PSS microfiber formation in an acidic coagulation bath, where the PEDOT:PSS microfiber is coagulated, whereas excess PSS chains are dissolved by the sulfuric acid solution
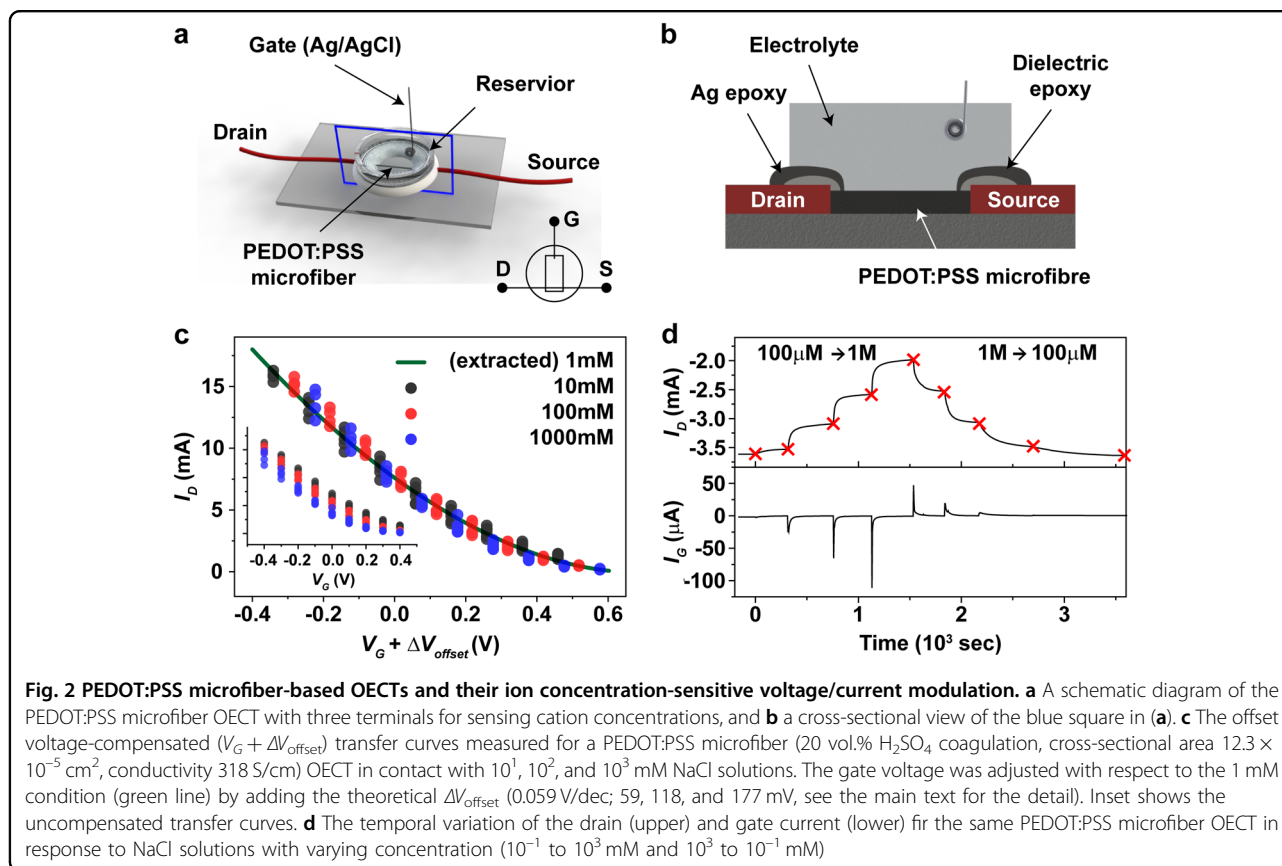
mass spectrometry, which was conducted at the Korea Polymer Testing and Research Institute (Koptri). For the repetitive measurement, the PEDOT:PSS fiber was washed out with 1 mM NaCl solution to reset the ion sensor.

Results and discussion

As mentioned in the Materials and methods section, PEDOT:PSS microfibers could be spun using a conventional wet-spinning process, as shown in Fig. 1a. Due to the rapid coagulation of PEDOT:PSS in the presence of sulfuric acid, the flow of the PEDOT:PSS solution injected through a syringe needle could be transformed into a continuous fiber-shaped PEDOT:PSS solid (Fig. 1b) having a circular/oval cross-section with a rough surface topography, as shown in the SEM images; the overall cross-sectional area of the solid could be controlled by changing the diameter of the needle and/or the acid concentration in the coagulation bath. Moreover, the PEDOT:PSS microfiber exhibited sufficient mechanical properties, such as a Young's modulus > 1.3 GPa and

tensile strength > 100 MPa, so that it could be successfully sewn into cotton fabric with a sewing needle (see Fig. S1 in the Supplementary Information). As depicted in Fig. 1c, PEDOT:PSS chains were rapidly coagulated in the strong acid bath, which could be attributed to the diffusion of water molecules and the dissolution of PSS chains. In this course, the excess amount of PSS chains, which minimally interact with the PEDOT chains, are removed and the crystallinity in PEDOT is enhanced[17]. Interestingly, as summarized in Table 1, although the conductivity (cross-sectional area) of the resultant PEDOT:PSS microfiber increased (decreased) with increased acid concentration, all microfibers showed similar values for the resistance per unit length. Considering that PSS is not conductive and that the total amount of PEDOT chains at a unit microfiber length are invariant regardless of the coagulation bath, the above-mentioned result suggests that the resistance per unit length is mainly determined by the total amount of residual PEDOT chains per unit length in the microfiber and that the increased conductivity in the more concentrated bath is due to the reduced microfiber

Fig. 2 PEDOT:PSS microfiber-based OECTs and their ion concentration-sensitive voltage/current modulation. a A schematic diagram of the PEDOT:PSS microfiber OECT with three terminals for sensing cation concentrations, and **b** a cross-sectional view of the blue square in (**a**). **c** The offset voltage-compensated ($V_G + \Delta V_{offset}$) transfer curves measured for a PEDOT:PSS microfiber (20 vol.% H_2SO_4 coagulation, cross-sectional area 12.3×10^{-5} cm^2, conductivity 318 S/cm) OECT in contact with 10^1, 10^2, and 10^3 mM NaCl solutions. The gate voltage was adjusted with respect to the 1 mM condition (green line) by adding the theoretical ΔV_{offset} (0.059 V/dec; 59, 118, and 177 mV, see the main text for the detail). Inset shows the uncompensated transfer curves. **d** The temporal variation of the drain (upper) and gate current (lower) fir the same PEDOT:PSS microfiber OECT in response to NaCl solutions with varying concentration (10^{-1} to 10^3 mM and 10^3 to 10^{-1} mM)

cross-sectional area. More in-depth characterization at various microfiber preparation conditions is in progress.

For OECT fabrication, the schematic diagrams for a microfiber-based OECT and its cross-sectional view are depicted in Figs. 2a, b, respectively (see Materials and methods for more details). As the hydrophobic PEDOT chains were highly doped by the hydrophilic PSS chains, small ions could be forced into/out of the PEDOT:PSS network in the presence of a gate bias and/or surrounding aqueous small ions[33,34]. Therefore, the PEDOT chains could be dedoped (doped) by positive (negative) gate bias and/or high (low) ion concentration, so that the source-to-drain current through the PEDOT:PSS microfiber channel could be effectively modulated[12]. This phenomenon is demonstrated in the inset of Fig. 2c. In the case of a 100 mM NaCl solution, the drain current could be reduced along with the on-off current ratio of 10^2 for a gate bias swept from −0.4 to 0.4 V at a fixed drain voltage of −0.6 V. Furthermore, the transfer curves were shifted when the concentration of NaCl in the reservoir was changed. The transfer curve was shifted more negatively for higher salt concentrations since a higher concentration of small ions could interrupt the doped state more efficiently. This observation can be explained by the Nernst equation, with the modified transfer characteristics (I_D vs. V_G) in the linear region

($(V_G + V_{offset}) - V_D \ll V_P$) described by:[16,23]

$$I_D = G\left(1 - \frac{V_G + V_{offset} - 1/2 V_D}{V_P}\right) \quad (1)$$

where G is the transconductance ($q\mu p_0 WT/L$), which can be determined from the electronic charge (q), mobility (μ), initial hole density (p_0), fiber dimensions (e.g., width (W), thickness (T), and length (L)), and gate (V_G)/drain voltages (V_D). In addition, V_P and V_{offset} are the pinch-off and offset voltages, which are described as qp_0/C_V and $A + kT/ne\cdot\ln[M^{n+}]$, respectively. Here, C_V is the volumetric capacitance of PEDOT:PSS, and A, k, T, and M^{n+} are the electrode potential difference between the gate electrode and PEDOT:PSS, Boltzmann's constant, temperature, and the concentration of ionic species with charge (n), respectively. Note also that V_{offset} includes the effect of the electrolyte concentration-driven potential between the gate electrode and PEDOT:PSS for a certain electrolyte concentration. Indeed, the transfer curves at electrolyte concentrations of 10^1, 10^2, and 10^3 mM well match those obtained at the adjusted V_G with an offset voltage difference with respect to the 1 mM condition (ΔV_{offset} or 0.059 V/dec) of 59, 118, and 177 mV at 300 K, respectively, as shown in Fig. 2c. Next, the time-dependent drain and gate currents were monitored

when the concentration of the NaCl solution in the reservoir was changed (Fig. 2d). Although the gate and drain voltages were fixed at 0 and –0.1 V, respectively, to set the given OECT device in the linear region, the reservoir solution was replaced by fresh solution with a designated NaCl concentration (10^{-1}, 10^0, 10^1, 10^2, and 10^3 mM) in sequence followed by measurement of the source-drain current. The negative drain current increased immediately after adding a more concentrated NaCl solution (10^{-1} to 10^3 mM), but decreased immediately after adding a less concentrated NaCl solution (10^3 to 10^{-1} mM). Furthermore, the ion migration between the gate electrode and the PEDOT:PSS layer could also be monitored by I_G when the given reservoir solution was replaced by another. Although our electrical setup only permitted measurement of relatively slow current variations, the polarity switching in the gate current depends on the salt concentration increase or decrease, which implicates the opposite direction for ion migration during the dedoping/doping in the PEDOT:PSS microfiber[31].

As we have already mentioned, it is not simple to define the active channel dimensions (i.e., length, width, and diameter) in microfiber-shaped devices, which significantly affects the resultant device output/transfer characteristics, and, thus, their sensing reliability/reproducibility. Therefore, for further characterization of the PEDOT:PSS microfiber-based OECT, we defined the variation ratio for the drain current ($|\Delta I_D/I_{D0}|$) using the following equation in combination with Eq. 1:

$$\frac{I_{D0} - I_D}{I_{D0}} = S \log \frac{[M^{n+}]}{[M_0^{n+}]}$$
$$S = \frac{(kT/ne) \ln 10}{V_P - V_{0,offset} - V_G + 1/2 V_D} \tag{2}$$

where I_{D0} and I_D are the drain currents at the reference ($[M_0^{n+}]$) and target electrolyte concentrations ($[M^{n+}]$), respectively, and $V_{0,offset}$ is the offset voltage at the reference concentration (all experiments were conducted using the reference concentration of 1 mM, with I_{D0} extracted from the linear fitting (I_D *vs.* log$[M^{n+}]$) for concentrations ranging from 10^1 to 10^3 mM). Note that S, which is independent of the microfiber channel dimensions (i.e., channel length and width, see also Fig. S2 of the Supplementary Information), can be regarded as a performance parameter showing the sensitivity of the variation ratio of the drain current in response to the change in ion concentration. The inset of Fig. 3a shows that the current variation ratio was found to be almost linearly proportional to log$[M^{n+}]$ in the range of 10^1 and 10^3 mM, with the apparent non-linear behavior below 10 mM attributed to deviation from the boundary condition. It is noteworthy that the observed linear relationship with substantially high slopes in this concentration range

suggest that the PEDOT:PSS microfiber could be useful for sensing human sweat, which contains 10^1–10^2 mM NaCl (vide infra)[35,36]. Furthermore, further analysis was carried out to explain the effect of the coagulation medium on S in comparison with the theoretically predicted value. As shown in Fig. 3a, the slope (S) increased from 0.093 to 0.153/dec with decreasing acid concentration in the coagulation bath from 100 to 20 vol.%, indicating that the PEDOT:PSS microfiber fabricated in the 20 vol.%, sulfuric acid solution exhibits the highest device sensitivity. Next, we conducted a verification step by comparing the measured values with those theoretically derived from Eq. 2, and also fundamentally studied the origin of the sensitivity variation in different concentrations of coagulation medium. First, the $V_P - V_{0,offset}$, the only term related to the material properties that determine S, at the extant coagulation condition was acquired from the transfer curves in the saturation region ($(V_G + V_{offset}) - V_D \geq V_P$), as described below;[16]

$$I_D = \frac{G}{2V_P} \left[(V_G + V_{offset}) - V_P \right]^2 \tag{3}$$

The values for $V_P - V_{0,offset}$ could be extracted from the x axis intercept ($V_P - V_{offset}$) in a plot of the square root of I_D vs. V_G in the saturation regime ($V_D = -0.6$ V and $V_G = -0.8$–0.8 V, in 100 mM NaCl solution). Figure 3b shows that the $V_P - V_{0,offset}$ increased from 0.47 to 0.84 V as the acid concentration increased from 20 to 100 vol.%. Although there exist certain deviations from the theoretical S values due to the non-ideal behavior of $V_P - V_{0,offset}$, which could be caused by device hysteresis during the OECT operation, the theoretical S values still follows well the trend observed for the measured values. In addition, when more concentrated sulfuric acid solutions were employed for coagulating PEDOT:PSS microfibers, both carrier concentration (p) and volumetric capacitance (C_V) increased but the slope of the p increase was steeper than that of the C_V increase, as shown in Fig. 3c. It is noteworthy that p and C_V indicate how many cations are needed to fully dedope the PEDOT chains (i.e., the total hole density) and how many ions can be *effectively* stored at a given bias by injecting small cations into the PEDOT (hole):PSS(anion) pairs (i.e., the effective hole density available for dedoping), respectively[21]. As the microfibers with relatively high PEDOT/PSS ratios were formed in the more concentrated sulfuric acid bath, the higher number of PEDOT(hole):PSS(anion) pairs in the unit volume should increase both C_V and p. Nonetheless, as proposed in Fig. 3d, enhanced fiber crystallinity at a higher PEDOT to PSS ratio[17] and a resulting less efficient ion penetration should cause a more gradual/reluctant increase in C_V than p. All the above-mentioned results demonstrate that the relative composition and crystallinity of the microfibers can modulate the resultant ion sensitivity (S), V_P, p, and
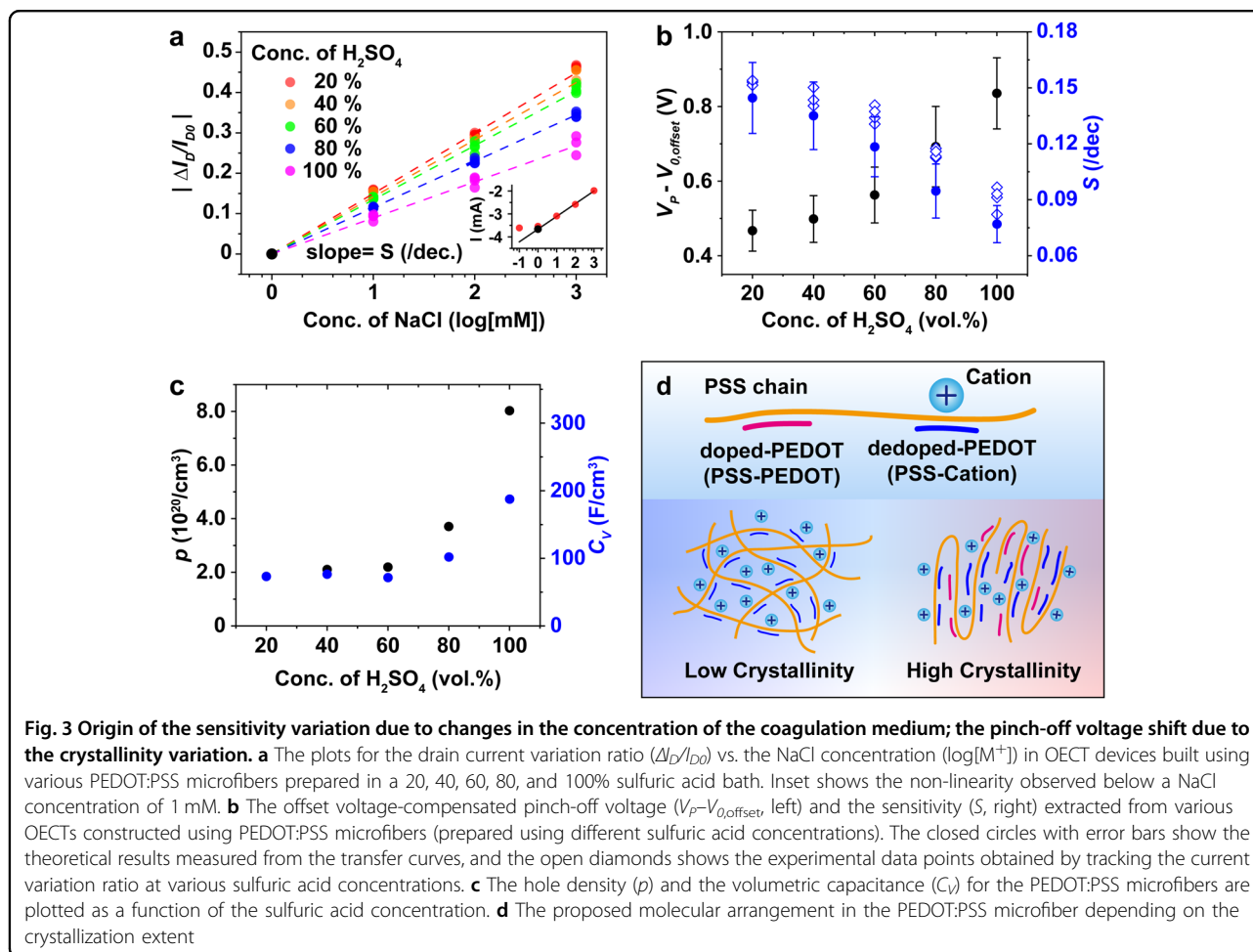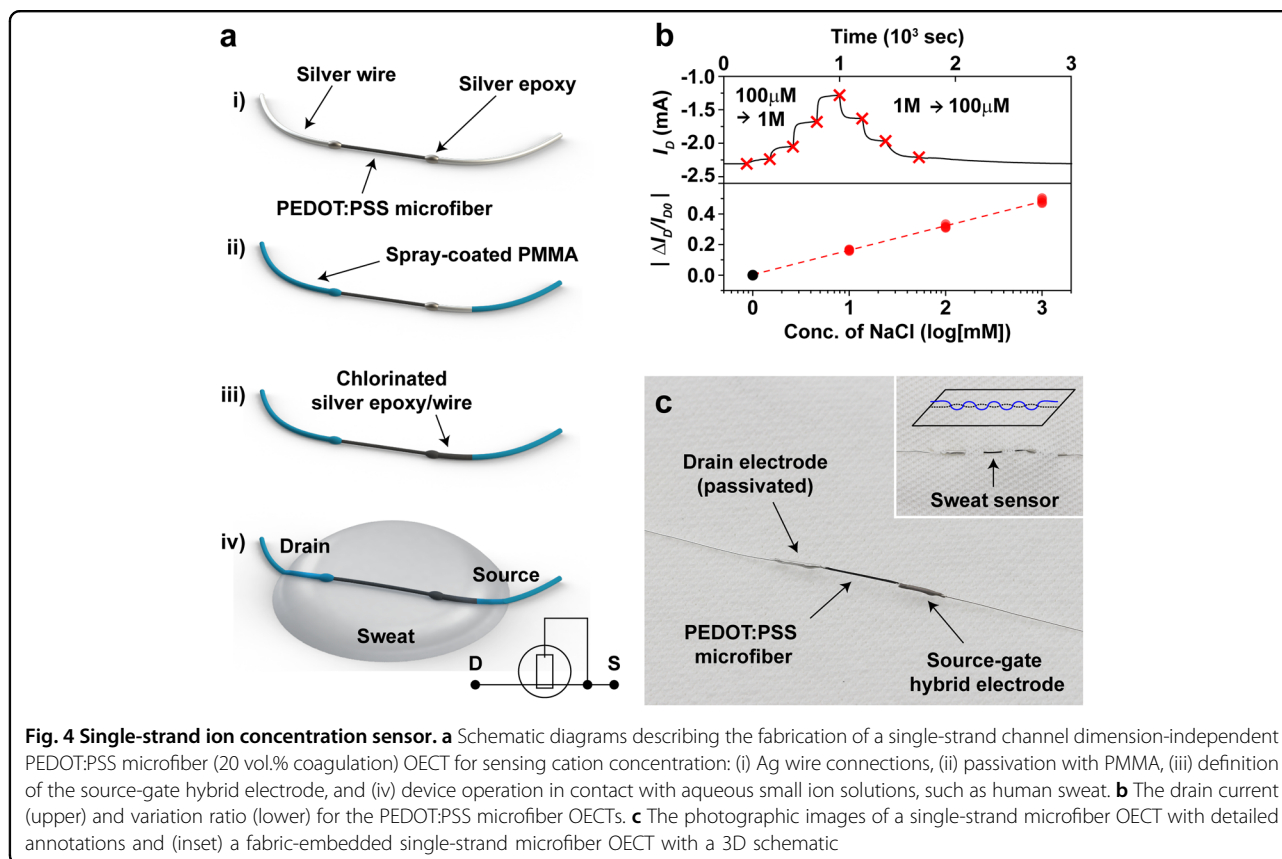
Fig. 3 Origin of the sensitivity variation due to changes in the concentration of the coagulation medium; the pinch-off voltage shift due to the crystallinity variation. a The plots for the drain current variation ratio ($\Delta I_D/I_{D0}$) vs. the NaCl concentration (log[M$^+$]) in OECT devices built using various PEDOT:PSS microfibers prepared in a 20, 40, 60, 80, and 100% sulfuric acid bath. Inset shows the non-linearity observed below a NaCl concentration of 1 mM. **b** The offset voltage-compensated pinch-off voltage (V_P–$V_{0,\text{offset}}$, left) and the sensitivity (S, right) extracted from various OECTs constructed using PEDOT:PSS microfibers (prepared using different sulfuric acid concentrations). The closed circles with error bars show the theoretical results measured from the transfer curves, and the open diamonds shows the experimental data points obtained by tracking the current variation ratio at various sulfuric acid concentrations. **c** The hole density (p) and the volumetric capacitance (C_V) for the PEDOT:PSS microfibers are plotted as a function of the sulfuric acid concentration. **d** The proposed molecular arrangement in the PEDOT:PSS microfiber depending on the crystallization extent

C_V. Note also that both the microfiber and thin-film PEDOT:PSS OECTs exhibit almost identical behavior for the pinch-off voltage shift and sensitivity variation (see Fig. S3 in the Supplementary Information).

For practical applications, particularly, toward human-friendly wearable electronics, two-terminal single-strand fiber-type devices are more convenient than conventional three-terminal devices in terms of device architecture. Therefore, we developed two-terminal-based single-strand OECT-based ion sensors. The fabrication procedure is depicted in Fig. 4a. (i) Both ends of the PEDOT:PSS microfiber were connected with Ag wires by coating the connection points with silver epoxy for the source and drain contacts. (ii) The active channel was defined by passivating the non-channel region with spray-coated PMMA layers except for one of the silver epoxy-coated connections. (iii) The unpassivated silver epoxy was chlorinated using Clorox 4% solution, with the resultant Ag/AgCl connected with the source side of the PEDOT:PSS channel functioning as a source-gate hybrid electrode. Note that, in this configuration for the OECT, the role of this source-gate hybrid electrode, which is

equivalent to zero gate bias with respect to the source, is to apply only an electrolyte concentration-driven potential to the PEDOT:PSS channel, regardless of the dimension and position of the chlorinated silver connection[37]. As a result, an effective gate bias of 0 V can be applied to the PEDOT:PSS microfiber channel in contact with the electrolyte, whereas the ion concentration can be measured by monitoring the current variation ratio. This freestanding single-strand OECT is supposed to support an identical ion-sensing mechanism to that found for the conventional three-terminal OECT platform at zero gate bias, as shown in the circuit diagram of Fig. 4a. In fact, when the channel current was recorded using PEDOT:PSS microfibers with the maximum ion sensitivity (coagulated with the 20% sulfuric acid solution, $V_D = -0.1$ V) and different electrolyte solutions with ion concentration ranging from 10^{-1} to 10^3 mM, the behavior observed for I_D in Fig. 4b was equivalent to that observed for the three-terminal ion sensor shown in Fig. 2d. In addition, the measured sensitivity (0.16/dec) is identical to that found for the three-terminal PEDOT:PSS OECT shown in Fig. 3a. Furthermore, although the diameter of the

Fig. 4 Single-strand ion concentration sensor. a Schematic diagrams describing the fabrication of a single-strand channel dimension-independent PEDOT:PSS microfiber (20 vol.% coagulation) OECT for sensing cation concentration: (i) Ag wire connections, (ii) passivation with PMMA, (iii) definition of the source-gate hybrid electrode, and (iv) device operation in contact with aqueous small ion solutions, such as human sweat. **b** The drain current (upper) and variation ratio (lower) for the PEDOT:PSS microfiber OECTs. **c** The photographic images of a single-strand microfiber OECT with detailed annotations and (inset) a fabric-embedded single-strand microfiber OECT with a 3D schematic

PEDOT:PSS fiber was sufficiently small (10–100 μm), the fiber itself was relatively durable, leading to successful incorporation into conventional fabric (Fig. 4c).

Finally, we demonstrated the feasibility of employing single-strand substrate-free OECTs to human-friendly wearable electronics by sensing the total small ion concentration in various samples, including human sweat. Figure 5a shows that the microfiber-based OECT can be easily attached onto a human arm, suggesting that this single-strand fiber-type ion sensor can be mounted onto a wrist guard or embedded into clothes due to its small size and flexibility. Furthermore, as body fluids such as extracellular fluid or sweat mainly consist of sodium ions with a dominant portion of over 90% (see Fig. 5b)[35,36,38], which falls into the reliable ion detection range for the PEDOT:PSS microfiber OECT (see Fig. 3), it is expected that, in principle, our microfiber-based ion sensor can monitor the concentration of major cations in human sweat once a calibration curve is obtained. Therefore, we demonstrated that a single-strand OECT-based ion sensor can be employed for measuring the cation concentration in PBS solution, artificial sweat, and, finally, human sweat samples. First, the single-strand OECT was prepared by the aforementioned fabrication procedure, and then the calibration curve was obtained by linearly fitting a $(I_{D0}-I_D)/I_{D0}$ vs.

log $[M^{n+}]$ plot (Fig. 5c). Then, the experimentally measured drain current variation ratio ($\Delta I_D/I_{D0}$) was converted into the corresponding cation concentration, which was cross-checked with the value measured by IC-ICP mass spectrometry. As shown in Fig. 5d, the cation concentrations measured with the OECT sensor for the PBS, artificial sweat (detailed composition were described in Materials and methods section), and human sweat samples matched well those obtained from IC-ICP within 3% error. However, the human sweat sample showed a relatively large error of ~10%. Considering that human sweat includes not only monovalent cations (e.g., Na^+, K^+) but also other divalent cations (e.g., Ca^{2+}, Zn^{2+}, Cu^{2+}, Fe^{2+}, Ni^{2+}, etc.), all of which can be detected by IC-ICP, we suspect that our OECT-based sensor, which mainly interacts with all monovalent small cations regardless of charge, showed am underestimated value compared with that obtained from IC-ICP. Furthermore, Fig. 5e shows that the microfiber OECT can perform repetitive measurement of cation concentrations after washing out with the 1 mM NaCl solution.

Conclusions

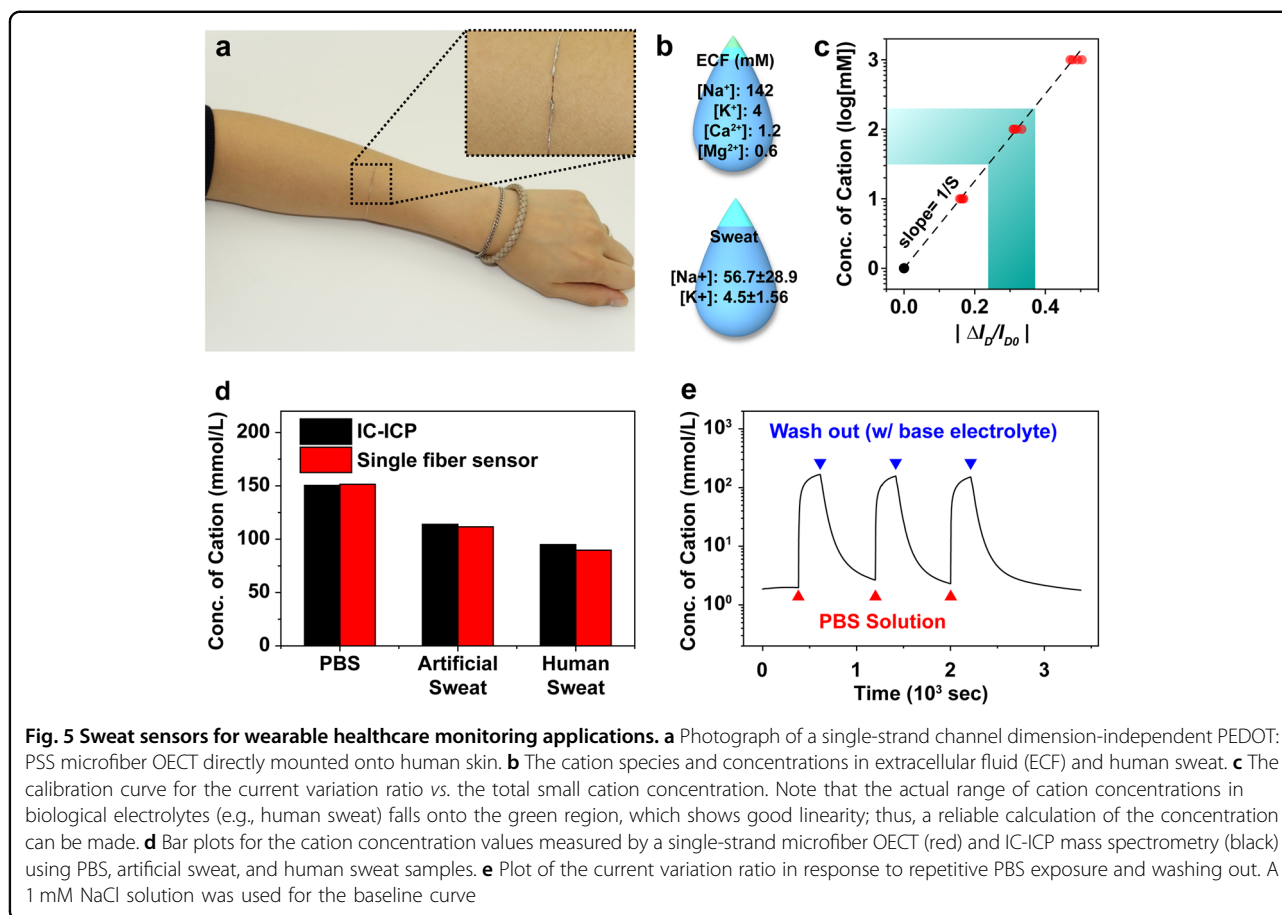In this study, we developed single-strand fiber-type channel dimension-independent wearable ion

Fig. 5 Sweat sensors for wearable healthcare monitoring applications. a Photograph of a single-strand channel dimension-independent PEDOT: PSS microfiber OECT directly mounted onto human skin. **b** The cation species and concentrations in extracellular fluid (ECF) and human sweat. **c** The calibration curve for the current variation ratio *vs.* the total small cation concentration. Note that the actual range of cation concentrations in biological electrolytes (e.g., human sweat) falls onto the green region, which shows good linearity; thus, a reliable calculation of the concentration can be made. **d** Bar plots for the cation concentration values measured by a single-strand microfiber OECT (red) and IC-ICP mass spectrometry (black) using PBS, artificial sweat, and human sweat samples. **e** Plot of the current variation ratio in response to repetitive PBS exposure and washing out. A 1 mM NaCl solution was used for the baseline curve

concentration sensors based on a PEDOT:PSS microfiber OECT. Due to the aqueous stable but reliable microfiber channel material composed of crystallized PEDOT:PSS obtained via sulfuric acid treatment and the novel characterization method relying on the current variation ratio, the PEDOT:PSS microfiber OECT-based sensors were able to be used to measure the concentration of aqueous small cations even without defining the exact channel dimensions. Finally, we developed single-strand fibrillar OECTs by introducing a source-gate hybrid electrode and demonstrated that the resultant channel dimension-independent microfiber sensors were able to perform real-time repetitive measurements of the total cation concentrations in human sweat samples, which indicates that it is highly feasible to apply this novel but very simple device platform based on free-standing conducting polymer microfibers to human-friendly wearable electronics.

Author details
[1]School of Materials Science and Engineering, Gwangju Institute of Science and Technology, Gwangju 61005, Republic of Korea. [2]Department of Physics, Kyonggi University, Suwon, Gyeonggi-Do 16227, Republic of Korea. [3]Advanced Institutes of Convergence Technology, Seoul National University, Suwon, Gyeonggi-Do 16229, Republic of Korea

Conflict of interest
The authors declare that they have no conflict of interest.

Publisher's note
Springer Nature remains neutral with regard to jurisdictional claims in published maps and institutional affiliations.

References
1. Yuen, J. D., Walper, S. A., Melde, B. J., Daniele, M. A. & Stenger, D. A. Electrolyte-sensing transistor decals enabled by ultrathin microbial nanocellulose. *Sci. Rep.* **7**, 40867 (2017).
2. Gualandi, I. et al. Textile organic electrochemical transistors as a platform for wearable biosensors. *Sci. Rep.* **6**, 33637 (2016).

3. Ludwig, K. A., Uram, J. D., Yang, J., Martin, D. C. & Kipke, D. R. Chronic neural recordings using silicon microelectrode arrays electrochemically deposited with a poly(3,4-ethylenedioxythiophene) (PEDOT) film. *J. Neural Eng.* **3**, 59 (2006).

4. Xiao, Y. et al. Electrochemical polymerization of poly(hydroxymethylated-3,4-ethylenedioxythiophene) (PEDOT-MeOH) on multichannel neural probes. *Sens. Actuators B: Chem.* **99**, 437–443 (2004).

5. Kozai, T. D. Y. et al. Ultrasmall implantable composite microelectrodes with bioactive surfaces for chronic neural interfaces. *Nat. Mater.* **11**, 1065–1073 (2012).

6. Ganji, M. et al. Development and translation of PEDOT:PSS microelectrodes for intraoperative monitoring. *Adv. Funct. Mater.* **28**, 1700232 (2017).

7. Sessolo, M. et al. Easy-to-fabricate conducting polymer microelectrode arrays. *Adv. Mater.* **25**, 2135–2139 (2013).

8. Koutsouras, D. A. et al. PEDOT:PSS microelectrode arrays for hippocampal cell culture electrophysiological recordings. *MRS Commun.* **7**, 259–265 (2017).

9. Guo, L., Ma, M., Zhang, N., Langer, R. & Anderson, D. G. Stretchable polymeric multielectrode array for conformal neural interfacing. *Adv. Mater.* **26**, 1427–1433 (2014).

10. Khodagholy, D. et al. Highly conformable conducting polymer electrodes for in vivo recordings. *Adv. Mater.* **23**, H268–H272 (2011).

11. Campana, A., Cramer, T., Simon, D. T., Berggren, M. & Biscarini, F. Electrocardiographic recording with conformable organic electrochemical transistor fabricated on resorbable bioscaffold. *Adv. Mater.* **26**, 3874–3878 (2014).

12. Khodagholy, D. et al. High transconductance organic electrochemical transistors. *Nat. Commun.* **4**, ncomms3133 (2013).

13. Rivnay, J. et al. High-performance transistors for bioelectronics through tuning of channel thickness. *Sci. Adv.* **1**, e1400251 (2015).

14. Khodagholy, D. et al. In vivo recordings of brain activity using organic transistors. *Nat. Commun.* **4**, 1575 (2013).

15. Leleux, P. et al. Organic electrochemical transistors for clinical applications. *Adv. Healthc. Mater.* **4**, 142–147 (2015).

16. Bernards, D. A. & Malliaras, G. G. Steady-state and transient behavior of organic electrochemical transistors. *Adv. Funct. Mater.* **17**, 3538–3544 (2007).

17. Kim, N. et al. Highly conductive PEDOT:PSS nanofibrils induced by solution-processed crystallization. *Adv. Mater.* **26**, 2268–2272 (2014).

18. Wei, Q., Mukaida, M., Naitoh, Y. & Ishida, T. Morphological change and mobility enhancement in PEDOT:PSS by adding co-solvents. *Adv. Mater.* **25**, 2831–2836 (2013).

19. Worfolk, B. J. et al. Ultrahigh electrical conductivity in solution-sheared polymeric transparent films. *Proc. Natl. Acad. Sci. USA* **112**, 14138–14143 (2015).

20. Liu, Y. et al. High-performance flexible all-solid-state supercapacitor from large free-standing graphene-PEDOT/PSS films. *Sci. Rep.* **5**, 17045 (2015).

21. Proctor, C. M., Rivnay, J. & Malliaras, G. G. Understanding volumetric capacitance in conducting polymers. *J. Polym. Sci. Part B: Polym. Phys.* **54**, 1433–1436 (2016).

22. Sessolo, M., Rivnay, J., Bandiello, E., Malliaras, G. G. & Bolink, H. J. Ion-selective organic electrochemical transistors. *Adv. Mater.* **26**, 4803–4807 (2014).

23. Lin, P., Yan, F. & Chan, H. L. W. Ion-sensitive properties of organic electrochemical transistors. *ACS Appl. Mater. Interfaces* **2**, 1637–1641 (2010).

24. Loi, A., Manunza, I. & Bonfiglio, A. Flexible, organic, ion-sensitive field-effect transistor. *Appl. Phys. Lett.* **86**, 103512 (2005).

25. Zhang, M. et al. Highly sensitive glucose sensors based on enzyme-modified whole-graphene solution-gated transistors. *Sci. Rep.* **5**, srep08311 (2015).

26. Khodagholy, D. et al. Organic electrochemical transistor incorporating an ionogel as a solid state electrolyte for lactate sensing. *J. Mater. Chem.* **22**, 4440–4443 (2012).

27. Gualandi, I. et al. Textile organic electrochemical transistors as a platform for wearable biosensors. *Sci. Rep.* **6**, srep33637 (2016).

28. Okuzaki, H., Harashina, Y. & Yan, H. Highly conductive PEDOT/PSS microfibers fabricated by wet-spinning and dip-treatment in ethylene glycol. *Eur. Polym. J.* **45**, 256–261 (2009).

29. Jalili, R., Razal, J. M., Innis, P. C. & Wallace, G. G. One-step wet-spinning process of poly(3,4-ethylenedioxythiophene):poly(styrenesulfonate) fibers and the origin of higher electrical conductivity. *Adv. Funct. Mater.* **21**, 3363–3370 (2011).

30. Jalili, R., Razal, J. M. & Wallace, G. G. Wet-spinning of PEDOT:PSS/Functionalized-SWNTs composite: a facile route toward production of strong and highly conducting multifunctional fibers. *Sci. Rep.* **3**, srep03438 (2013).

31. Tarabella, G. et al. A single cotton fiber organic electrochemical transistor for liquid electrolyte saline sensing. *J. Mater. Chem.* **22**, 23830–23834 (2012).

32. Coppedè, N. et al. Human stress monitoring through an organic cotton-fiber biosensor. *J. Mater. Chem. B* **2**, 5620–5626 (2014).

33. Stavrinidou, E. et al. Direct measurement of ion mobility in a conducting polymer. *Adv. Mater.* **25**, 4488–4493 (2013).

34. Rivnay, J. et al. Structural control of mixed ionic and electronic transport in conducting polymers. *Nat. Commun.* **7**, 11287 (2016).

35. Patterson, M. J., Galloway, S. D. R. & Nimmo, M. A. Variations in regional sweat composition in normal human males. *Exp. Physiol.* 85, 869–875 (2000).

36. Sonner, Z. et al. The microfluidics of the eccrine sweat gland, including biomarker partitioning, transport, and biosensing implications. *Biomicrofluidics* **9**, 031301 (2015).

37. Tarabella, G. et al. Effect of the gate electrode on the response of organic electrochemical transistors. *Appl. Phys. Lett.* **97**, 123304 (2010).

38. Hall, J. E. *Guyton and Hall Textbook of Medical Physiology* (Elsevier Health Sciences, Philadelphia, PA, USA, 2016).